

Nonlinear Thomas-Fermi-Poisson theory of screening for a Hall bar under strong magnetic fields

A. Siddiki and Rolf R. Gerhardts

Max-Planck Institut für Festkörperforschung, Heisenbergstrasse 1, D-70569 Stuttgart, Germany

Abstract. Low-temperature screening properties of the inhomogeneous two-dimensional electron gas in a Hall bar subjected to a strong perpendicular magnetic field are explored using a self-consistent approach. An external oscillating modulation potential with an amplitude of the order of the cyclotron energy is added to the electron-confining background potential, and the resulting change of the self-consistent potential is investigated as function of modulation strength, magnetic field, and temperature. The consequences of Landau-level pinning and the interplay of compressible and incompressible regions for the resulting strongly non-linear screening phenomena are explained.

1. Introduction

As a consequence of the highly degenerate, Landau-quantised energy levels, a two-dimensional electron gas (2DEG) in a strong perpendicular magnetic field has unusual low-temperature screening properties [1, 2]. In an inhomogeneous 2DEG with long-range density fluctuations, pinning of Landau levels (LLs) leads to quasi metallic regions with high density of states (DOS) at the Fermi energy and therefore nearly perfect screening ability. These so called “compressible” regions coexist with quasi-insulating “incompressible” regions separating compressible regions with different LLs at the Fermi energy. In the incompressible regions the Fermi energy falls into the gap between two adjacent LLs and, in thermodynamic equilibrium at low temperatures, no redistribution of electrons is possible which could contribute to screening. Also, in the incompressible regions the electron density $n_{el}(\mathbf{r})$ is constant, corresponding to total filling of an integer number of LLs, while in the compressible regions $n_{el}(\mathbf{r})$ adjusts itself so that the self-consistent electrostatic potential energy $V(\mathbf{r})$ of an electron differs from the Fermi energy, more precisely from the constant electrochemical potential μ^* by a Landau energy $\hbar\omega_c(n + 1/2)$, where $\omega_c = eB/m$ is the cyclotron frequency in the magnetic field B . As a consequence, $V(\mathbf{r})$ differs between different compressible regions by integer multiples of $\hbar\omega_c$. Landau level pinning and the interplay of compressible and incompressible regions will strongly affect the screening properties of the 2DEG.

In a bounded 2D geometry with translation invariance in one direction, the compressible and incompressible regions degenerate to strips parallel to the boundary. For half-space and Hall-bar geometries models with planar charge distributions have been proposed that allow closed solutions of Poisson’s equation, i.e., the calculation of the potential for given electron density, and estimates of position and widths of the incompressible strips have been given [3, 4]. By adding the non-linear Thomas-Fermi approximation for the calculation of the electron density from the potential, that work was extended to a self-consistent approach which allows to calculate both electron density and electrostatic potential for arbitrary temperature [5, 6]. This approach shows that the existence and the width of incompressible strips depends sensitively on temperature. It also permits to calculate their position and width

for given background charges without additional assumptions. We adopt this approach to investigate systematically the screening of a harmonic external potential in such a confined 2DEG.

2. The Thomas-Fermi-Poisson (TFP) approach

In order to employ the approach presented in Ref. [6], we assume that our 2DEG lies in the $z = 0$ plane, laterally confined by in-plane gates located at $x < -d$ and $x > d$, which are kept at voltages V_L and V_R , respectively. In this work we assume a symmetric depletion on both sides with the depleted strips having a width of $|d - b|$, and we will consider only symmetric potentials $V(-x) = V(x)$, notably with $V(\pm d) = V_L = V_R = 0$, which leave the electron density profile symmetric, $n_{el}(-x) = n_{el}(x)$. Then, solution of Poisson's equation yields for the electrostatic potential energy of an electron

$$V(x) = -\frac{2e}{\bar{\kappa}} \int_{-d}^d dt K(x, t) \rho(t), \quad K(x, t) = \ln \left| \frac{\sqrt{(d^2 - x^2)(d^2 - t^2)} + d^2 - tx}{(x - t)d} \right|, \quad (1)$$

where $\rho(x)$ is the surface charge density in the strip $|x| < d$ and $\bar{\kappa}$ is an average dielectric constant [6]. If we assume a homogeneous surface density n_0 of positive background charges, $\rho(x) = e[n_0 - n_{el}(x)]$, we obtain

$$V(x) = V_{bg}(x) + V_H(x), \quad \text{where} \quad V_{bg}(x) = -E_0 \sqrt{1 - (x/d)^2} \quad (2)$$

with $E_0 = 2\pi e^2 n_0 d / \bar{\kappa}$ is the confining potential due to the background and $V_H(x)$ the Hartree contribution due to the electron density, given by Eq. (1) with $\rho(x)$ replaced by $-en_{el}(x)$. Assuming that $V(x)$ varies on a characteristic length much larger than typical quantum lengths, notably the magnetic length $l_m = \sqrt{\hbar/eB}$, one can calculate $n_{el}(x)$ for given $V(x)$ in the Thomas-Fermi approximation [6]

$$n_{el}(x) = \int dE D(E) f([E + V(x) - \mu^*]/k_B T), \quad \text{with} \quad f(\epsilon) = [1 + e^\epsilon]^{-1} \quad (3)$$

the Fermi function, μ^* the electrochemical potential and T the temperature. Here $D(E)$ is the density of states of the 2DEG, which we take to be the bare spin-degenerate Landau DOS,

$$D(E) = (\pi l_m^2)^{-1} \sum_{n=0}^{\infty} \delta(E - \hbar\omega_c(n + 1/2)). \quad (4)$$

This completes the TFP scheme for the self-consistent calculation of $n_{el}(x)$ and $V(x)$ for given temperature and magnetic field and homogeneous background charge. To study screening effects, we add to $V_{bg}(x)$ in Eq. (2) the harmonic external potential

$$V_m(x) = V_0 \cos(k_\lambda x), \quad \text{with} \quad k_\lambda = (\lambda + 1/2)\pi/d, \quad (5)$$

where λ is an integer (to preserve the boundary conditions), calculate the resulting self-consistent potential and electron density as function of the modulation strength V_0 , and compare these results with those for $V_0 = 0$. [In principle $V_m(x)$ can be generated by a redistribution of the background charge density.]

For technical reasons we always start the iterative solution of the self-consistent TFP scheme with a calculation for vanishing temperature and magnetic field and for homogeneous background, i.e., we take $n_{el}(x) = D_0[E_F - V(x)]\theta(E_F - V(x))$ with $D_0 = m/\pi\hbar^2$ as 2D DOS and define the symmetric density profile by the requirement $V(b) = V(-b) = E_F = \mu^*(T = 0)$. Then Eq. (1) reduces to a linear integral equation,

$$V(x) = -E_0 \sqrt{1 - \left(\frac{x}{d}\right)^2} + \frac{1}{\pi a_0} \int_{-b}^b dt [E_F - V(t)] K(x, t) \quad (6)$$

with $a_0 = \bar{\kappa}/2\pi e^2 D_0$ the bare screening length. [Due to a misprint, in the corresponding Eq. (15) of Ref. [6] the factor π in the denominator is missing.] The choice of b defines the average density, which is then kept fixed for the calculations at finite temperature, magnetic field, and modulation.

3. Results and discussion

In the numerical calculations we keep some parameters fixed. So we divide the interval $-d < x < d$ into 500 subintervals and calculate $V(x)$ and $n_{el}(x)$ on the corresponding equidistant mesh points $x = x_n$. The depletion length is defined by taking $b/d = 0.9$ and the bar width by $\pi a_0/d = 0.01$. For GaAs values ($\bar{\kappa} = 12.4$) $a_0 \approx 5$ nm, this means $2d \approx 3$ μ m, which is small compared to typical Hall bars used in experiments. Calculation for smaller a_0/d , i.e., larger d requires more subintervals, and thus larger storage and computation time, to achieve the same accuracy near the incompressible strips, but yields no qualitative changes. Therefore, we fix the mentioned parameter values and obtain from the solution of the system of linear equations defined by Eq. (6) an average electron density that yields the average LL filling factor $\bar{\nu} = 2$ for a cyclotron energy $\hbar\omega_c = \Omega_2 \equiv 0.2311 \times 10^{-2} E_0$. Starting from this solution we find the solution of the non-linear TFP scheme at finite T and B implementing the Newton-Raphson method [5, 6]. For the bare modulation potential (5) we take $\lambda = 2$, so that $V_m(x)$ has a maximum at $x = 0$ and two minima at $x = \pm 0.4d$, i.e. well inside the Hall bar, whereas near the maxima at $x = \pm 0.8d$ the confinement potential increases strongly and the electron density starts to decrease, so that the screening properties are obscured by boundary effects.

Figure 1 shows the potentials and electron densities of the Hall bar calculated for several modulation amplitudes at strong magnetic fields and low temperatures. On the left panel we consider the case $V_0 = 0$ and show the temperature dependence in the inset, while the right panel shows the evolution of the potential and electron density with increasing modulation amplitude. All the electron densities are expressed in terms of local filling given by $\nu(x) = 2\pi n_{el}(x) l_m^2$ and potentials are normalised by E_0 .

Figure 1a presents the electron density, with two incompressible strips located symmetrically near $x/d = \pm 0.75$ and the surrounding compressible regions. With decreasing temperature the incompressible strips are stronger pronounced (see inset Fig. 1a) and so are the related potential steps (inset Fig. 1b). As mentioned in the introduction, in compressible regions one of the LLs is pinned at μ^* , leading to nearly perfect screening and constant potential, while in an incompressible region μ^* falls into a gap between the LLs making redistribution of electrons, and hence screening, energetically impossible and $n_{el}(x)$ constant. We demonstrate these features in Fig. 1b, where we exhibit μ^* (dash-dotted line), the first two LLs (dashed lines with opaque circles), and the total potential (solid line).

In the right panels we show electron density and potential profiles for various modulation amplitudes V_0 at a low temperature and a high magnetic field, at which the average filling factor in the centre region is around 2.5, i.e., the $n = 1$ LL is pinned to μ^* . With increasing V_0 the external potential (energy) is raised in the centre and lowered near $x/d = \pm 0.4$, which leads to a lowering of $n_{el}(x)$ near $x = 0$ and an increase near $x/d = \pm 0.4$. This redistribution of charges screens the potential at the low temperature of Fig. 1c,d so effectively, that the resulting weak modulation of the self-consistent potential for $V_0/E_0 = 0.01$ and 0.02 is not seen on the scale of Fig. 1d. At larger modulation, however, the filling factor $\nu(0)$ in the centre falls below 2, which means that near $x = 0$ the self-consistent potential must rise so much that the lowest LL $n = 0$ reaches μ^* (as is demonstrated for $V_0/E_0 = 0.07$ in Fig. 1d). Therefore, on both sides of the centre region incompressible strips must develop across which the self-consistent potential changes by $\hbar\omega_c$.

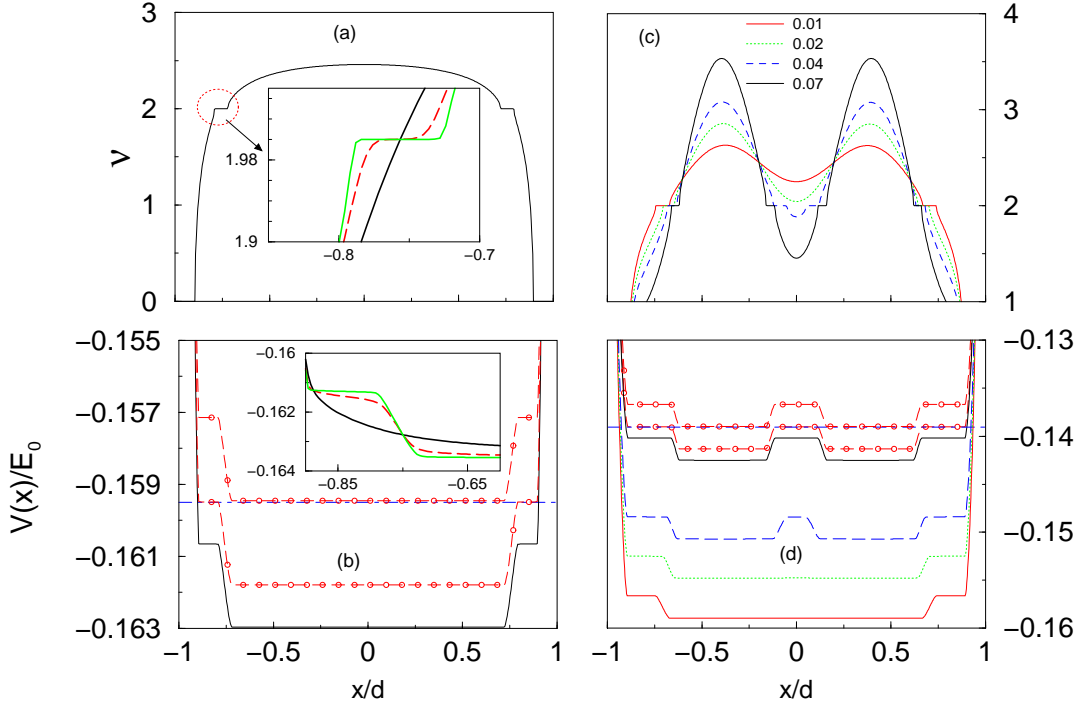


Figure 1. Electron densities [(a),(c)] and electrostatic potentials $V(x)$ [(b),(d)] without modulation [(a),(b)] and with external modulation potential $V_m(x) = V_0 \cos(qx)$, $q = 2.5\pi/d$ [(c),(d)], where V_0/E_0 values are given by the legend. Insets in (a) and (c) demonstrate the temperature dependence for $kT/E_0 = 0.1 \times 10^{-3}$ (thick solid line), 0.2×10^{-4} (dashed line), and 0.1×10^{-4} (thin solid line).

We see from these results that the screening is highly non-linear, since the change of the self-consistent potential produced by the harmonic modulation (5) is step-like rather than cosine-like. Moreover, for weak modulation $V_0/E_0 \lesssim 0.02$ the resulting variation $\Delta V = V(0) - V(0.4d)$ of the self-consistent potential is so small that it is not detectable on the scale of Fig. 1d, whereas ΔV for $V_0/E_0 \gtrsim 0.04$ assumes the constant value $\hbar\omega_c$. Apparently this stepwise increase of ΔV with V_0 is a consequence of the pinning of LLs to the electrochemical potential (locally perfect screening), which is stronger pronounced at lower temperatures. We now consider this effect in more detail.

3.1. Tuning the modulation strength at fixed magnetic fields

In Fig. 2a we show the “variance” of the screened potential as function of the amplitude V_0 of the applied modulation for several values of the magnetic field and a fixed low temperature, and in Fig. 2b the same dependence for a fixed value of the cyclotron energy and several temperatures. We define this variance as the difference between the maximum (at $x = 0$) and the minimum (near $x = 0.4d$) of the difference $V(x; V_0) - V(x; 0)$ of the self-consistent potentials calculated with and without modulation, respectively.

For a fixed value of the magnetic field (i.e., of $\Omega \equiv \hbar\omega_c$), we obtain a stepwise increasing curve, as we expect from the discussion of Fig. 1c,d, which corresponds to $\Omega = \Omega_2$. The corresponding (thick solid) curve in Fig. 2a shows two broadened steps around $V_0/E_0 = 0.025$ and 0.075 . We have already discussed the reason for the step at the lower V_0 value and for the plateaus below and above this step. With further increasing V_0 the filling factor near the density maxima becomes larger than 4 (see Fig. 1c) while the density in the centre is still finite. Then new incompressible strips with local filling $\nu(x) = 4$ develop on both sides of the density maxima, which corresponds to a decrease of the self-consistent potential by

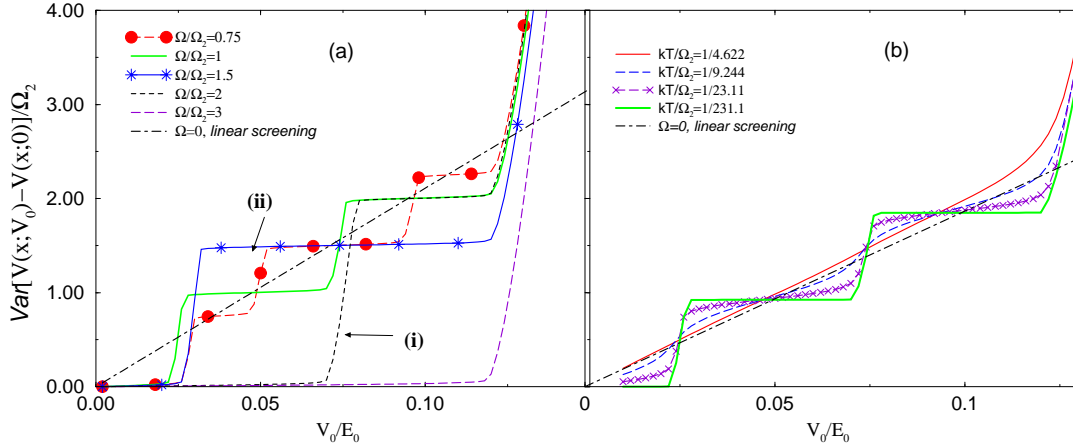


Figure 2. (a) Variance of screened potential versus amplitude V_0 of the external potential for various magnetic field values ($\pi a_0/d = 0.01$, $k_B T/E_0 = 2 \cdot 10^{-5}$). The dash-dotted line indicates linear screening for zero B and T , see text. (b) Temperature dependence of the variance for $\Omega/\Omega_2 = 1$

the amount Ω to new local minima near $x = \pm 0.4d$. In Fig. 2a this leads to the plateau of height 2Ω . As V_0 increases further, the electron density $n_{el}(0)$ in the centre vanishes and no further redistribution of electrons from the centre region to the region of maximum density is possible. Then the high screening ability of the electron system breaks down and the variance increases with further increasing V_0 much more rapidly (see behaviour at $V_0/E_0 > 0.125$). This breakdown happens for $\Omega = \Omega_2$ when the filling factor at the density maxima is somewhat larger than 4 (~ 5).

We can now understand all the curves in Fig. 2a. Since, apart from the fine structure near incompressible strips, the global density profile depends only weakly on the magnetic field, for the lowest curve (long-dashed, $\Omega = 3\Omega_2$) typical filling factors $\nu(x)$ are by a factor 3 smaller than for the case $\Omega = \Omega_2$ we have just discussed. Therefore the breakdown situation is reached when the filling factor near the density maxima is of the order $5/3 < 2$. Thus the breakdown sets in before an incompressible strip and thus a plateau of height $3\Omega_2$ of the variance can develop. For $\Omega = 2\Omega_2$ [short-dashed line, label (i)] the local filling factors $\nu(x)$ are typically about half as large as in the case $\Omega = \Omega_2$. Thus, $\nu(x) < 2$ for weak modulation, and incompressible strips with $\nu(x) = 2$ can occur only near the density maxima for sufficiently strong modulation, and a single plateau of height $2\Omega_2$ occurs below the breakdown regime. A similar situation is met for $\Omega = 1.5\Omega_2$ [label (ii)], but since now $\nu(x)$ is about $2/3$ times that for $\Omega = \Omega_2$, the threshold of the plateau is reached at a considerably weaker modulation. Finally, for $\Omega = 0.75\Omega_2$ we obtain three plateaus in the pre-breakdown regime, corresponding to the successive development of incompressible strips with local filling factor 4 (maxima), 2 (minimum), and 6 (maxima).

We should mention that the behaviour of the variance curves is not always that regular. For special values of Ω it may happen that incompressible strips near the centre and near the density maxima occur at the same modulation strength. Then steps of height 2Ω occur. We met such a situation for $\Omega = 0.5\Omega_2$ (not shown in Fig. 2a), which yields nearly the same trace as $\Omega = \Omega_2$.

For the smaller Ω values, the variance curves oscillate around the dash-dotted line in Fig. 2a, which represents the corresponding result $2V_0/[E_0\epsilon(q)]$ of linear Thomas-Fermi screening [1] for zero T and B , with $\epsilon(q) = 1 + 1/(a_0q) = 41$ for $q = 2.5\pi/d$. This linear screening approximation breaks down when the amplitude of the screened potential (i.e. half

the variance) becomes equal to the Fermi energy of the unmodulated system [7], which can be estimated from Fig. 1 as $\sim 3 \times 10^{-3} E_0$, corresponding to $V_0 \sim 0.12 E_0$. Finally we should mention that the small-variance regime in Fig. 2a also corresponds to linear screening, but now with $\varepsilon(q) = 1 + (D_T/D_0)/(a_0 q)$, where D_T is the thermodynamic DOS in a LL, which can be estimated by $D_T/D_0 \sim \hbar\omega_c/(4k_B T)$ [1]. Thus, the slope of the variance curves is by a factor $\sim 4k_B T/\Omega \ll 1$ smaller than that of the dash-dotted line.

As shown in Fig. 2b, with increasing temperature the plateaus of the variance-versus- V_0 curves get a finite slope and the steps are smeared out. This is an immediate consequence of the temperature dependence of the incompressible strips (see Fig. 1a). At the highest shown temperature screening becomes again linear and independent of B , but now the temperature is so high that the thermodynamic DOS is noticeably smaller than D_0 . A clear indication of steps is seen only for $k_B T/\hbar\omega_c \lesssim 1/25$ [5].

3.2. Sweeping the magnetic field at fixed modulation strength

From the above considerations we expect that, for fixed modulation strength V_0 , the variance as a function of the cyclotron energy Ω will mainly follow integer multiples of Ω with abrupt transitions between neighbouring integers corresponding to the steps in Fig. 2a. These abrupt transitions will be similar to the familiar magnetic-field-dependent jumps of the chemical potential of a homogeneous 2DEG at fixed density, which have nothing to do with the periodic modulation and should be separated from the modulation-induced structures. To this end, we first discuss the chemical potential.

In a Hall bar with spatially varying electron density and electrostatic fields the electrochemical potential μ^* is a thermodynamic quantity being constant in equilibrium. As an analogue of the chemical potential of a homogeneous 2DEG we define $\mu(x) = \mu^* - V(x)$ and denote in the following $\mu(0)$ as the chemical potential. In Fig. 3a we show, together with the LLs $\Omega(n + 1/2)$, a plot of $\mu(0)$ versus Ω , which exhibits a saw-tooth shape as known from the unbounded 2DEG. To understand this, we plot in Fig. 3b and 3c filling factor and self-consistent potential $V(x)$ for four magnetic field values marked in Fig. 3a. For the lowest selected B value [opaque circle in Fig. 3a, label (i)], in the centre region the LL with $n = 1$ is pinned to μ^* , the filling in the centre is $\nu(0) > 2$, and the incompressible strips with $\nu(x) = 2$ are close to the edges. As Ω increases these strips move towards the centre, and the compressible centre region, with $\nu(x) > 2$ and a flat potential minimum, shrinks [case (ii), filled square]. In the transition region at still larger Ω [(iii), opaque diamond] the strips merge to an incompressible centre region, where the potential minimum is no longer flat, and its depth (measured from the adjacent compressible strips) is smaller than Ω . As Ω sweeps through the transition region, the width of the incompressible centre region and the depth of the potential minimum shrink to zero. When the transition is completed [(iv), filled triangle], we have again a broad compressible centre region in which the next lower LL (here $n = 0$) is pinned to μ^* . Thus, in the confined 2DEG in a Hall bar, the jump of the chemical potential from a LL to the next lower one is realised by a drastic change of the position dependence of the self-consistent potential, which in our idealised model happens in the centre.

To separate these effects from the modulation-induced screening effects, we define now the variance of the self-consistent potential as $var = V(0) - V(x_{min})$, where $\pm x_{min} \sim \pm 0.4d$ are the positions of the minima of $V(x)$ in the presence of modulation, and $V(0)$ is the local maximum at the centre. In Fig. 4a we plot var versus Ω , together with $\mu(0)$. As expected, var follows widely integer multiples of Ω , whereas $\mu(0)$ follows half-integer ones. But, whereas $\mu(0)$ jumps with increasing Ω always to the next lower LL, var can also jump to a higher multiple of Ω . To understand this, we show in Fig. 4b-4e density and potential profiles for the six Ω values marked in Fig. 4a.

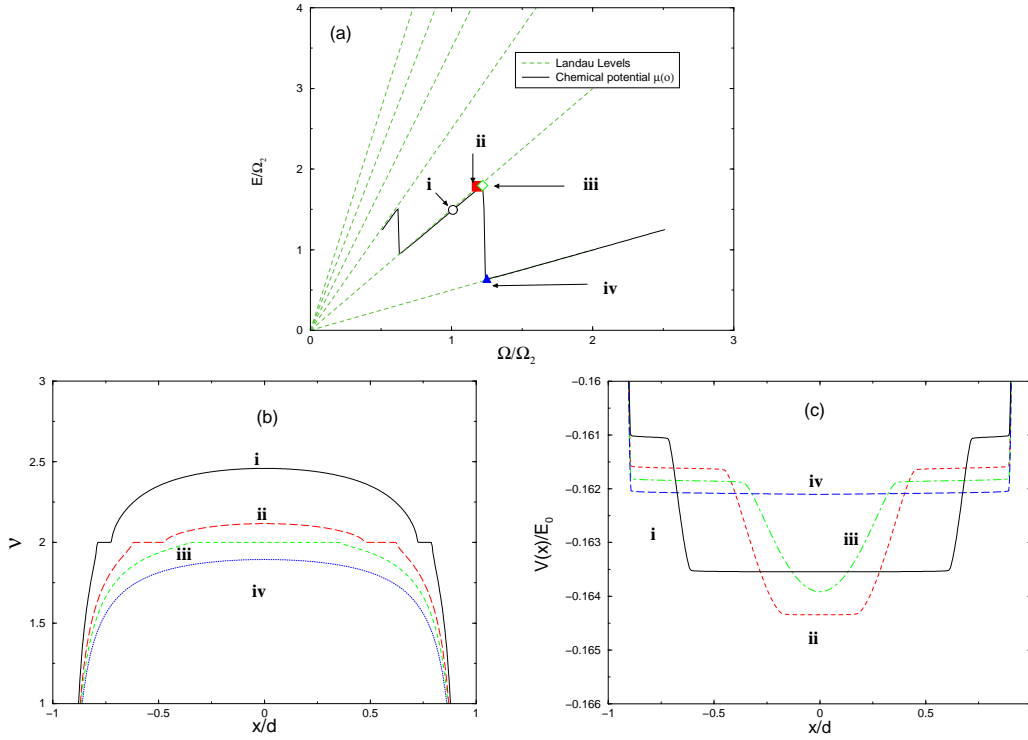


Figure 3. Chemical potential and LLs (a); selected density (b) and potential (c) profiles.

In case (i) (solid lines in Fig. 4b and 4c) the centre region is compressible with $\nu(0)$ slightly larger than 2 and with the $n = 1$ LL pinned to μ^* , whereas the compressible regions near the density maxima have $\nu(x) > 4$ ($\nu(x_{min}) \approx 5$) and the $n = 2$ LL is pinned to μ^* . This yields $var \approx \Omega$. For slightly larger Ω [(ii), dashed lines in 4b and 4c], an incompressible strip with filling factor 2 and a local maximum of $V(x)$ at $x = 0$ develops in the centre, while the situation near the density maxima is unchanged. This leads to $\Omega < var < 2\Omega$. At still slightly larger Ω [(iii), dotted lines in 4b and 4c], the region near the density maxima is still qualitatively unchanged, whereas in the centre a compressible region with $\nu(x) < 2$ develops, where the $n = 0$ LL is pinned to μ^* , leading to $var \approx 2\Omega$. As Ω increases further [(iv) – (vi)], the situation in the centre remains qualitatively the same, whereas the filling factor at the density maxima changes from $\nu(x_{min}) > 4$ to $\nu(x_{min}) < 4$, so that the incompressible strips with $\nu(x) = 4$ merge [(v), dashed lines in 4d and 4e] and finally disappear, accompanied by the disappearance of the potential step across these strips. Thus, we have again $var \approx \Omega$, until for much larger Ω the maximum filling factor becomes smaller than 2 and var goes back to the very small value corresponding to linear screening in the lowest Landau level.

In summary, the low-temperature screening properties of a confined inhomogeneous 2DEG in strong magnetic fields can be understood from a few basic facts: Incompressible regions with integer values of the local filling factor (even integer values for a spin-degenerate 2DEG), and thus constant electron density, are accompanied by steps of the self-consistent potential between the adjacent compressible regions, where adjacent Landau levels are pinned to the constant electrochemical potential, so that the step height is $\hbar\omega_c$, the cyclotron energy. The modulation-induced variation of the self-consistent potential (“variance”) is, therefore, usually an integer multiple of $\hbar\omega_c$ and changes by $\pm\hbar\omega_c$ if incompressible regions appear or disappear (near local maxima or minima of the electron density) due to a variation of modulation strength or magnetic field. Screening of the applied modulation potential breaks

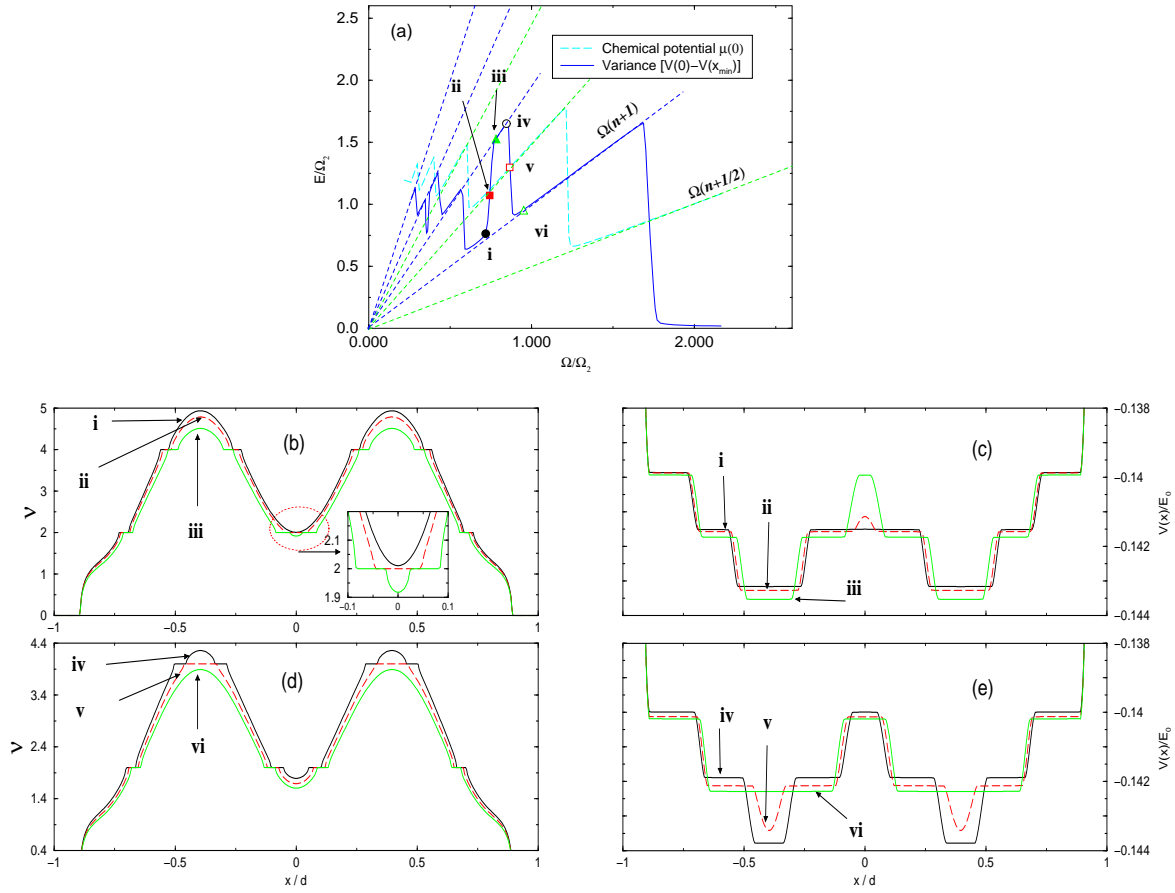


Figure 4. (a) Variance of self-consistent potential for modulation amplitude $V_0 = 0.05E_0$ versus Ω ; (b),(d) density and (c),(e) potential profiles for selected Ω values marked in (a). $k_B T/E_0 = 2 \cdot 10^{-5}$, $\pi a_0/d = 0.01$.

down if the electron density near the density minima becomes so small that no further redistribution of electrons from the local potential maxima to the local potential minima is possible.

Acknowledgements

We gratefully acknowledge helpful discussions with E. Ahlswede and J. Weis, and financial support by the Deutsche Forschungsgemeinschaft, SP “Quanten-Hall-Systeme” GE306/4-1.

References

- [1] Wulf U, Gudmundsson V, and Gerhardt R R, 1988 Phys. Rev. B 38 4218
- [2] Efros A L Solid State Commun. 1988 67 1019
- [3] Chklovskii D B, Shklovskii B I, and Glazman L I, 1992 Phys. Rev. B 46 4026
- [4] Chklovskii D B, Matveev K A, and Shklovskii B I, 1993 Phys. Rev. B 47 12605
- [5] Lier K and Gerhardt R R, 1994 Phys. Rev. B 50 7757
- [6] Oh J H and Gerhardt R R, 1997 Phys. Rev. B 56 13519
- [7] Wulf U and Gerhardt R R, 1988 Springer Series in S.State Sci. 83 162